CHINESE OPTICS LETTERS

Vol. 20, No. 5 | May 2022

High laser damage threshold $LiNa_5Mo_9O_{30}$ prism: for visible to mid-infrared range

Xiaoli Du (杜晓利)[1], Zeliang Gao (高泽亮)[1*], Lijuan Chen (陈丽娟)[2], Youxuan Sun (孙友轩)[1], and Xutang Tao (陶绪堂)[1**]

[1] State Key Laboratory of Crystal Materials, Shandong University, Jinan 250100, China

[2] School of Physics Science, University of Jinan, Jinan 250022, China

*Corresponding author: gaozeliang@sdu.edu.cn

**Corresponding author: txt@sdu.edu.cn

Received January 3, 2022 | Accepted March 1, 2022 | Posted Online March 24, 2022

In this study, an excellent polarization optical crystal $LiNa_5Mo_9O_{30}$ with wide transmission range and high laser damage threshold was researched in detail. The laser damage threshold of the $LiNa_5Mo_9O_{30}$ crystal was measured to be 2.64 GW/cm^2, which was the highest among polarized optical crystals. The birefringence in the range of 0.435–5 μm was larger than 0.14, while the wedge angle between 31.94° and 32.12° would satisfy the application in this waveband. The extinction ratio of the fabricated prism with the wedge angel of 31.09° was larger than 15,000:1. The results show that the $LiNa_5Mo_9O_{30}$ prism is an excellent polarization device, especially in the mid-infrared range and high-power applications.

Keywords: Glan prism; laser damage threshold; birefringence; polarized optical crystal.

DOI: 10.3788/COL202220.051602

1. Introduction

Polarized prisms have been widely used in laser modulation, optical information processing, imaging systems, and so on[1–6]. Birefringence is one of the crystal's physical properties and the basic requirement of polarized materials[7]. The performance of the polarized prism is directly determined by the polarized optical crystal. Large birefringence is the most important characteristic for the polarized optical crystal influencing prism fabrication. In addition, the transmission window of the polarized crystal determines the application range of the prism. So far, the calcite ($CaCO_3$), YVO_4, and α-BaB_2O_4 (α-BBO) are the widely used polarized optical crystals[8–10]. $CaCO_3$ is a kind of natural ore with birefringence of 0.1744 at 532 nm, which is the most famous polarized optical crystal. The $CaCO_3$ prism is of high performance, but it can only be used in the range of 0.35–2.3 μm[11]. What is more, the $CaCO_3$ crystal is difficult to grow due to its complete cleavage. Both YVO_4 and α-BBO crystals can be grown by the Czochralaki technique. The YVO_4 crystal has a relatively large birefringence of 0.2331 at 532 nm, and the prism can be used in the range of 0.5–4 μm. The α-BBO crystal exhibits a relatively small birefringence of 0.1241 at 532 nm, but its ultraviolet cut-off edge extends to 190 nm. Recently, biaxial crystals have been studied as polarized optical materials. The biaxial crystal α-$BaTeMo_2O_9$ (α-BTM) prisms have been realized successfully[6]. The α-BTM prisms with wedge angles of 28° and 28.6° can be used in the range of 0.4–3 μm and 0.5–5 μm, respectively. It means that there is not an angle for the α-BTM prism that is applicable for the range of 0.4–5 μm due to the refractive index dispersion of α-BTM. The α-BTM crystal is grown by the flux method whose growth rate is much lower than the Czochralski technique. Therefore, polarized optical crystals that can be quickly grown by the Czochralski technique with large birefringence, wide transmission window, and high laser damage threshold have attracted our attention.

The $LiNa_5Mo_9O_{30}$ crystal is a novel functional crystal, which was first, to the best of our knowledge, studied as a nonlinear optical crystal[12]. It crystallizes in the orthorhombic system, with space group Fdd2 and lattice constants $a = 7.2229(11)$ Å (1 Å = 0.1 nm), $b = 37.150(6)$ Å, $c = 17.954(3)$ Å, and $Z = 4$. The $LiNa_5Mo_9O_{30}$ crystal can be grown by the top-seeded solution growth method and Czochralski technique, and both the crystal quality and crystal growth rate can be satisfied[12–14]. The crystal has a wide transmission band (0.31–5.35 μm), covering the whole visible, near-infrared, and mid-infrared wavelength range. The refractive index dispersion curves from 0.4502 to 1.0626 μm exhibit that the $LiNa_5Mo_9O_{30}$ crystal has a large birefringence (0.2545 at 0.4502 μm), which is much larger than that of $CaCO_3$ and α-BBO[6,8,9,15]. The $LiNa_5Mo_9O_{30}$ crystal also exhibits no dissociation and suitable hardness of 5.2[14]. It is worth noting that the $LiNa_5Mo_9O_{30}$ crystal has a high laser damage threshold, which means it can be used in high-power lasers. Therefore, we considered that the $LiNa_5Mo_9O_{30}$ crystal should be a potential polarized optical crystal with wide transmission band and high laser damage threshold.

Laser damage threshold is an important parameter of the optical crystals and devices. High laser damage threshold is beneficial to high-power applications. The energy band and thermal stability of the crystal would affect its laser damage threshold. In addition, defects and impurities of the crystal could lower the laser damage threshold. Since the laser damage threshold is measured by a well-polished crystal plate, the processing quality of the crystal surface would affect this index. The surface absorption of the crystal is generally much larger than the body absorption; thus, the crystal surface damage threshold is usually much lower than the body damage threshold[16]. Therefore, we measured the laser damage threshold of the $LiNa_5Mo_9O_{30}$ crystal in this work.

In this paper, the laser damage threshold of the $LiNa_5Mo_9O_{30}$ crystal was measured to be 2.64 GW/cm^2 at 1064 nm with a pulse width of 10 ns and a pulse repetition of 1 Hz. The refractive index and birefringence were determined and obtained in the range from 0.435 μm to 5 μm, and a $LiNa_5Mo_9O_{30}$ prism can apply for this waveband with the wedge angle of 31.94°–32.12°. The extinction ratio of the prism we manufactured was 15,000:1, while the wedge angle was 31.09°.

2. Experimental Section and Result

In this work, a well-polished 4 mm × 4 mm × 1 mm (100)-faced crystal plate of $LiNa_5Mo_9O_{30}$ was employed to measure the laser damage threshold. The measurement was tested by a diode-pumped Nd:$Y_3Al_5O_{12}$ (Nd:YAG) nano-second laser (Minilite ll, Continuum) at the wavelength of 1064 nm with a pulse width of 10 ns and a pulse repetition of 1 Hz. The pump pulse energy was operated at around 35 mJ. Under the action of the constant pulsed laser, the crystal was moved until the gray spot appeared. The result shows that $LiNa_5Mo_9O_{30}$ has a high laser damage threshold of 2.64 GW/cm^2, which is much larger than that of $CaCO_3$ (300–600 MW/cm^2), YVO_4 (~1 GW/cm^2), α-BBO (~1 GW/cm^2), and α-BTM (~350 MW/cm^2)[17–20]. This means that $LiNa_5Mo_9O_{30}$ is a potential material for high-power practical applications.

The refractive indices dispersion of the $LiNa_5Mo_9O_{30}$ crystal was measured by the minimum deviation technique in the range of 0.435–2.325 μm at twelve discrete wavelengths. Two prisms of the $LiNa_5Mo_9O_{30}$ crystal were required, as shown in Fig. 1. The prisms were designed and processed with vertex angles of 23.6° and 21.5°, respectively. The refractive index determination manifests that $LiNa_5Mo_9O_{30}$ is a negative biaxial crystal. The refractive index axes X, Y, and Z are parallel to the crystallography axes a, c, and b, respectively. The refractive index dispersion curves at 0.435–2.325 μm are shown in Fig. 2. The Sellmeier equations are listed as follows:

$$n_x^2 = 3.21637 + 0.04103/(\lambda^2 - 0.06306) - 0.00631\lambda^2, \quad (1)$$

$$n_y^2 = 3.82713 + 0.08012/(\lambda^2 - 0.03836) - 0.00367\lambda^2, \quad (2)$$

$$n_z^2 = 3.91313 + 0.08738/(\lambda^2 - 0.06202) - 0.01374\lambda^2. \quad (3)$$

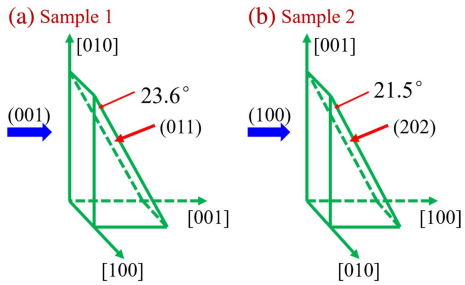

Fig. 1. Design of the two prisms.

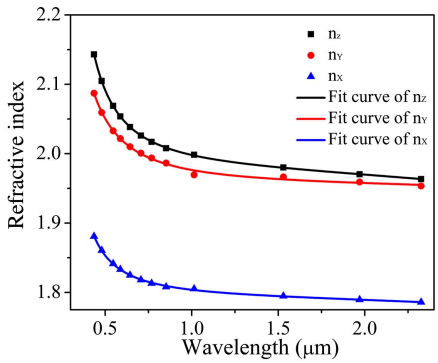

Fig. 2. Refractive index dispersion curves for the $LiNa_5Mo_9O_{30}$ crystal.

With the incident light along the Y axis of the biaxial crystal, the light will separate into components polarized along the X and Z axes, respectively. Then, the largest birefringence at certain wavelengths is obtained as $\Delta n = n_z - n_x$. According to experimental data and Sellmeier equations, the refractive index, birefringence, and critical angles of $LiNa_5Mo_9O_{30}$ are obtained and calculated in the range of 0.435–5 μm, as shown in Table 1. The largest birefringence is 0.26322 at 0.435 μm, which is larger than that of most crystals such as $CaCO_3$ and α-BBO.

According to the measured data and Sellmeier equations, the total internal reflection angles (α) are listed in Table 1 by using the following formula:

$$\alpha = \arcsin \frac{n_2}{n_1}, \quad (4)$$

where n_1 and n_2 are the refractive indices of the air and polarized light along the optic principal axis in the $LiNa_5Mo_9O_{30}$ crystal, respectively.

As shown in Fig. 3(a), when the crystal wedge plates of $LiNa_5Mo_9O_{30}$ with wedge angles $\theta = 31.94° - 32.12°$ were bonded by an air gap for the prism, the light polarized along the Z axis will be totally reflected, and the output light is polarized along the X axis, which would satisfy the application of 0.435–5 μm. In our experiment, the wedge angle was processed as 31.09°, as shown in Figs. 3(b) and 3(c).

As shown in Fig. 4, the extinction ratio was measured. A Nd:YAG laser operating at 1064 nm was used as laser resources.

Table 1. Refractive Index of Polarized Light in $LiNa_5Mo_9O_{30}$ Crystal and Total Internal Reflection Angles (α).

Wavelength (μm)	n_x	α for n_x (°)	n_z	α for n_z (°)	Δn
0.435	1.8807412	32.12075	2.1430628	27.815238	0.262322
0.480	1.8606013	32.51094	2.1047378	28.367070	0.244137
0.546	1.8414265	32.89200	2.0689064	28.904238	0.22748
0.587	1.8332104	33.05823	2.0537403	29.138112	0.220530
0.643	1.8248497	33.22925	2.0384182	29.378478	0.213569
0.706	1.8180732	33.36927	2.0260654	29.575333	0.207992
0.768	1.8131116	33.47259	2.0170307	29.721084	0.203919
0.852	1.8080104	33.57955	2.0077730	29.872016	0.199763
1.014	1.8051898	33.63900	1.9983893	30.026666	0.193200
1.529	1.7947450	33.86115	1.9800734	30.333462	0.185328
1.970	1.7894868	33.97419	1.9703647	30.498796	0.180878
2.325	1.7858615	34.05261	1.9633567	30.619331	0.177495
3	1.7788370	34.20566	1.9491655	30.866540	0.170329
3.5	1.7727272	34.34000	1.9370040	31.081793	0.164277
4	1.7658269	34.49310	1.9232193	31.329669	0.157392
4.5	1.7580749	34.66686	1.9076748	31.614292	0.149600
5	1.7494329	34.86284	1.8902735	31.939532	0.140841

A polarizer was used to modulate the light polarization direction. The silicon photocell was used to transfer the light into current, and then the signal was detected by a galvanometer. When the direction of light propagated through the polarizer is perpendicular to the Z direction, the weakest polarized light was detected. On the contrary, the strongest polarized light

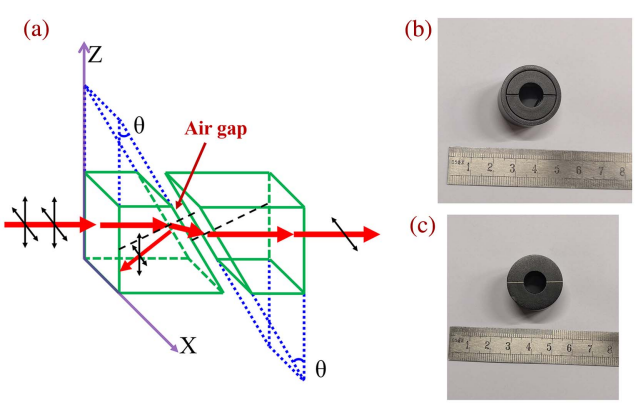

Fig. 3. (a) Illustration of light propagation in the $LiNa_5Mo_9O_{30}$ prism; (b) and (c) prisms of the $LiNa_5Mo_9O_{30}$ crystal.

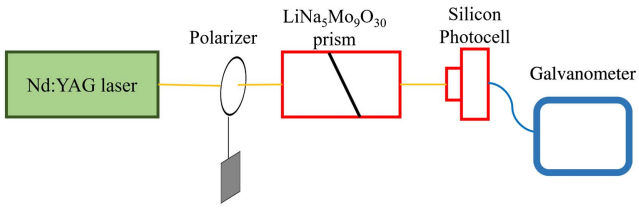

Fig. 4. Schematic of the extinction ratio measurement.

was obtained with the light polarization along the X direction. The extinction ratio of the prism was measured as larger than 15,000:1, which can satisfy the experiment requirements.

3. Discussion

The properties of the widely used polarization optical crystals are listed in Table 2. The birefringence of $CaCO_3$ and α-BBO crystals is smaller than that of other crystals, but both exhibit excellent ultraviolet transmission properties, especially α-BBO crystals. In the ultraviolet-visible and near-infrared bands, $CaCO_3$ and α-BBO can mostly meet the requirements of the device applications. The YVO_4 crystal extends the mid-infrared edge to 4 μm, and exhibits a large birefringence. The YVO_4 crystal can be grown by the Czochralski technique, and its crystal growth speed is faster than that of α-BBO and α-BTM crystals. Unfortunately, the YVO_4 crystal cannot cover the entire mid-infrared range. The α-BTM crystal is the first polarization optical biaxial crystal, whose transmission range can cover the near- and mid-infrared range. Although the α-BTM crystal has a wide transmission range, the α-BTM prism should be designed with two wedge angles (28°/28.6°) to cover the application range of 0.4–3 μm and 0.5–5 μm, respectively. All of the laser damage thresholds of $CaCO_3$, α-BBO, YVO_4, and α-BTM crystals are lower than 1 GW/cm^2, which limits their application in high-power optics.

The $LiNa_5Mo_9O_{30}$ crystal not only shows larger birefringence than $CaCO_3$ and α-BBO, but also presents a wider transmission window than $CaCO_3$, α-BBO, and YVO_4. According to our calculations, the $LiNa_5Mo_9O_{30}$ crystal with wedge angles of $\theta = 31.94°–32.12°$ can cover 0.435–5 μm, which is better than the α-BTM prism. Due to the uniform melting property, high-quality $LiNa_5Mo_9O_{30}$ crystal can be grown by the top-seeded solution crystal growth method and the Czochralski technique with high growth rate, which is beneficial for device applications. In addition, the $LiNa_5Mo_9O_{30}$ prism is the first choice for high-power applications due to its high laser damage threshold.

4. Conclusion

In this paper, the laser damage threshold of the $LiNa_5Mo_9O_{30}$ crystal was determined to be 2.64 GW/cm^2. The refractive index and dispersion curves were determined and obtained in the range from 0.435 μm to 2.325 μm. The birefringence of $LiNa_5Mo_9O_{30}$ at 0.435 μm and 5 μm was determined and

Table 2. Properties of Widely Used Crystals for Prisms.

Crystal	$LiNa_5Mo_9O_{30}$	α-BTM	$CaCO_3$	YVO_4	α-BBO
Space group	Fdd2	$Pca2_1$	R-3c	$I4_1/amd$	R3c
Cleavage	No	No	Yes	No	No
Deliquescence	No	No	No	No	Yes
Birefringence	0.2305@532 nm 0.1852@1550 nm	0.24605@532 nm 0.2000@1550 nm	0.1744@532 nm 0.1564@1550 nm	0.2331@532 nm 0.2039@1550 nm	0.1241@532 nm 0.1202@1550 nm
Transmission range for prism	0.31–5.35 μm	0.4–5 μm	0.35–2.3 μm	0.5–4.0 μm	0.19–3.5 μm
Laser damage threshold	2.64 GW/cm^2	350 MW/cm^2	300–600 MW/cm^2	1 GW/cm^2	1 GW/cm^2

calculated to be 0.262322 and 0.140841, respectively. When the incident direction is along the Y axis, a prism with a wedge angle from 31.94° to 32.12° can realize light separation in the range of 0.435–5 μm. The Glan prism bonded by an air gap was designed using two $LiNa_5Mo_9O_{30}$ wedges with an angle of 31.09°. The extinction ratio of the prism was determined to be larger than 15,000:1. The results provide a promising high-power polarized prism ranging from the visible to mid-infrared region.

Acknowledgement

This work was supported by the National Natural Science Foundation of China (Nos. 51021062, 62175129, 50990061, and 50802054), 973 Program of China (No. 2010CB630702), China Postdoctoral Science Foundation (No. 20110491600), and Program of Introducing Talents of Disciplines to Universities in China (111 Program) (No. b06017).

References

1. V. Sankaran, M. J. Everett, D. J. Maitland, and J. T. Walsh, Jr., "Comparison of polarized-light propagation in biological tissue and phantoms," Opt. Lett. **24**, 1044 (1999).
2. G. Le Tolguenec, F. Devaux, and E. Lantz, "Two-dimensional time-resolved direct imaging through thick biological tissues: a new step toward noninvasive medical imaging," Opt. Lett. **24**, 1047 (1999).
3. J. M. Schmitt, A. H. Gandjbakhche, and R. F. Bonner, "Use of polarized light to discriminate short-path photons in a multiply scattering medium," Appl. Opt. **31**, 6535 (1992).
4. Z. Gao, X. Yin, W. Zhang, S. Wang, M. Jiang, and X. Tao, "Electro-optic properties of $BaTeMo_2O_9$ single crystal," Appl. Phys. Lett. **95**, 151107 (2009).
5. P. Kumar, A. I. Maydykovskiy, M. Levy, N. V. Dubrovin, and O. A. Aktsipetrov, "Second harmonic generation study of internally-generated strain in bismuth-substituted iron garnet films," Opt. Express **18**, 1076 (2010).
6. Z. L. Gao, Q. Wu, X. T. Liu, Y. X. Sun, and X. T. Tao, "Biaxial crystal alpha-$BaTeMo_2O_9$: theory study of large birefringence and wide-band polarized prisms design," Opt. Express **23**, 3851 (2015).
7. S. B. Mehta, M. Shribak, and R. Oldenbourg, "Polarized light imaging of birefringence and diattenuation at high resolution and high sensitivity," J. Opt. **15**, 094007 (2013).
8. R. Appel, C. D. Dyer, and J. N. Lockwood, "Design of a broadband UV-visible alpha-barium borate polarizer," Appl. Opt. **41**, 2470 (2002).
9. F. Wu, G. Li, J. Huang, and D. Yu, "Calcite/barium fluoride ultraviolet polarizing prism," Appl. Opt. **34**, 3668 (1995).
10. C. H. Huang, G. Zhang, M. Wei, L. X. Huang, X. J. Huang, and H. Y. Shen, "Investigation of several parameters in the design of YVO_4 polarizing prism," Opt. Commun. **224**, 1 (2003).
11. I. C. Olson, R. A. Metzler, N. Tamura, M. Kunz, C. E. Killian, and P. U. Gilbert, "Crystal lattice tilting in prismatic calcite," J. Struct. Biol. **183**, 180 (2013).
12. W. Zhang, H. Yu, J. Cantwell, H. Wu, K. R. Poeppelmeier, and P. S. Halasyamani, "$LiNa_5Mo_9O_{30}$: crystal growth, linear, and nonlinear optical properties," Chem. Mater. **28**, 4483 (2016).
13. V. A. Sukharev, A. P. Sadovskiy, E. A. Sukhanova, A. D. Dovnarovich, D. A. Spassky, K. M. Podurec, A. A. Kaloyan, V. Nagirnyi, S. I. Omelkov, and I. C. Avetissov, "Crystal growth and luminescent properties of $LiNa_5Mo_9O_{30}$," J. Cryst. Growth **519**, 35 (2019).
14. X. L. Du, Z. L. Gao, F. A. Liu, X. J. Guo, X. M. Wang, Y. X. Sun, and X. T. Tao, "Anisotropic properties and Raman spectra of a $LiNa_5Mo_9O_{30}$ single crystal grown by the TSSG method," Crystengcomm **22**, 7716 (2020).
15. G. Ghosh, "Dispersion-equation coefficients for the refractive index and birefringence of calcite and quartz crystals," Opt. Commun. **163**, 95 (1999).
16. S. Papernov, G. J. Exarhos, A. W. Schmid, D. Ristau, M. J. Soileau, and C. J. Stolz, "Laser-induced surface damage of optical materials: absorption sources, initiation, growth, and mitigation," Proc. SPIE **7132**, 71321J (2008).
17. S. Gangopadhyay, "Study of nonlinear optical phenomenon in BaB_2O_4," Nonlinear Opt. Quantum Opt. **48**, 177 (2017).
18. J. A. Piper and H. M. Pask, "Crystalline Raman lasers," IEEE J. Sel. Top. Quantum Electron. **13**, 692 (2007).
19. G. C. Bhar, A. K. Chaudhary, P. Kumbhakar, A. M. Rudra, and S. C. Sabarwal, "A comparative study of laser-induced surface damage thresholds in BBO crystals and effect of impurities," Opt. Mater. **27**, 119 (2004).
20. V. L. Borodin and I. V. Nefedova, "Growth and characteristics of calcite single crystals," J. Cryst. Growth **275**, e633 (2005).